Collective Dynamics in Optomechanical Arrays

Georg Heinrich,[1] Max Ludwig,[1] Jiang Qian,[2] Björn Kubala,[1] and Florian Marquardt[1,3]

[1]*Institute for Theoretical Physics, Universität Erlangen-Nürnberg, Staudtstr. 7, 91058 Erlangen, Germany*
[2]*Department of Physics, Center for NanoScience and Arnold Sommerfeld Center for Theoretical Physics, Ludwig-Maximilians-Universität München, Theresienstr. 37, D-80333 München, Germany*
[3]*Max Planck Institute for the Science of Light, Günther-Scharowsky-Straße 1/Bau 24, 91058 Erlangen, Germany*

(Received 24 September 2010; revised manuscript received 30 April 2011; published 20 July 2011)

Optomechanical systems couple light stored inside an optical cavity to the motion of a mechanical mode. Recent experiments have demonstrated setups, such as photonic crystal structures, that in principle allow one to confine several optical and vibrational modes on a single chip. Here we start to investigate the collective nonlinear dynamics in arrays of coupled optomechanical cells. We show that such "optomechanical arrays" can display synchronization, and that they can be described by an effective Kuramoto-type model.

DOI: 10.1103/PhysRevLett.107.043603 PACS numbers: 42.50.Wk, 07.10.Cm, 42.65.Sf

The emerging field of optomechanics seeks to explore the interaction between nanomechanics and light (see [1] for a recent review). Rapid progress in laser cooling of nanomechanical oscillators [2,3] promises new fundamental tests of quantum mechanics [4], while applications benefit from ultrasensitive detection of displacements, masses and forces [5–7]. Recently, the exciting concept of optomechanical crystals has been introduced [8–10], where defects in photonic crystal structures are used to generate both localized optical and mechanical modes that interact with each other. For instance, this opens the prospect of integrated optomechanical circuits combining several functions on a single chip (see also [11,12]). On a fundamental level, this raises questions concerning potential collective dynamics in systems consisting of many coupled optomechanical cells, which we will term optomechanical "arrays" [Figs. 1(a) and 1(b)]. Here we start to address this issue and explore, in particular, synchronization phenomena.

Any optomechanical system consists of a laser-driven optical mode (OM) whose frequency shifts in response to a mechanical displacement: $\delta\omega_{\mathrm{opt}} = -Gx$. For a laser red-detuned from the OM ($\Delta = \omega_{\mathrm{Laser}} - \omega_{\mathrm{opt}} < 0$), dynamical backaction effects induced by the finite photon decay time κ^{-1} lead to cooling of the mechanical motion. For blue detuning ($\Delta > 0$), antidamping results. Once this overcomes the internal mechanical friction, a Hopf bifurcation towards a regime of self-induced mechanical oscillations takes place [Fig. 1(c)] [13–18]. While the mechanical amplitude A is fixed, the oscillation phase φ is undetermined and, as we will see, may lock to external forces or to other optomechanical oscillators.

Synchronization has first been discovered by Huygens and is now recognized as an important feature of collective nonequilibrium behavior in fields ranging from physics over chemistry to biology and neuroscience [19]. A paradigmatic, widely studied model for synchronization was introduced by Kuramoto [20]. For two oscillators, his phase evolution equation reads $\dot{\varphi}_1 = \Omega_1 + K\sin(\varphi_2 - \varphi_1)$, and likewise for $\dot{\varphi}_2$. One finds synchronization ($\dot{\varphi}_1 = \dot{\varphi}_2$) if the coupling K exceeds the threshold $K_c = |\Omega_2 - \Omega_1|/2$, and the phase lag $\delta\varphi = \varphi_2 - \varphi_1$ vanishes for large K according to $\sin(\delta\varphi) = (\Omega_2 - \Omega_1)/2K$. For the globally coupled, mean-field type version of infinitely many oscillators, there is a phase transition towards synchronization beyond some threshold K_c that depends on the frequency distribution [21]. In many examples the Kuramoto model is found as a generic, reduced description of the phase dynamics. Nevertheless, for any specific system, it remains to be seen whether this model (or possibly a structurally similar variant thereof) applies at all, and how the coupling K is connected to microscopic parameters [22–24]. We now turn to this question in the case of optomechanical oscillators.

A single optomechanical cell consists of a mechanical mode (displacement x) coupled to a laser-driven OM (light amplitude α):

$$m\ddot{x} = -m\Omega^2 x - m\Gamma\dot{x} + \hbar G|\alpha|^2, \tag{1}$$

$$\dot{\alpha} = \left[i(\Delta + Gx) - \frac{\kappa}{2}\right]\alpha + \frac{\kappa}{2}\alpha_{\mathrm{max}}. \tag{2}$$

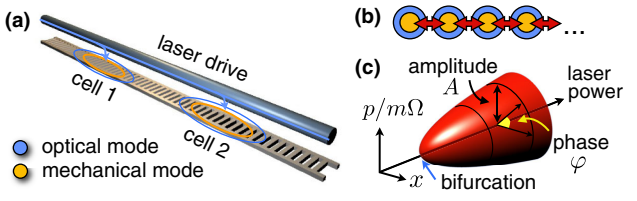

FIG. 1 (color online). Optomechanical crystals may be used to build arrays with several localized optical and mechanical modes. (a) Potential setup fabricated as a periodically patterned, freestanding dielectric beam on a chip with laser drive via tapered fibre as in [8,9]. (b) Schematic array of mechanically coupled optomechanical cells. (c) For a single cell, at sufficient laser drive power, there is a Hopf bifurcation towards self-induced mechanical oscillations with an undetermined phase φ.

Here, $F = \hbar G|\alpha|^2$ is the radiation pressure force, Ω the mechanical frequency, Γ the intrinsic damping, G the optomechanical frequency pull per displacement, and $\alpha_{\max}$ is the maximum light-field amplitude achieved at resonance (set by the laser input power).

Near the Hopf bifurcation [Fig. 1(c)], we choose as a starting point for our analysis the equations of a Hopf oscillator that describe the slow mechanical phase and amplitude dynamics [16] which result from integrating out the light field:

$$\dot{\varphi} = -\Omega + \frac{F(t)}{m\Omega A}\cos(\varphi), \tag{3}$$

$$\dot{A} = -\gamma(A - \bar{A}) + \frac{F(t)}{m\Omega}\sin(\varphi). \tag{4}$$

In this Hopf model, $\bar{A}$ describes the steady-state amplitude, and γ is the rate at which perturbations will relax back to $\bar{A}$. Moreover, we have introduced an external force $F(t)$ (as added to Eq. (1)). The dependence of γ, $\bar{A}$ on the microscopic parameters can be deduced by expanding the average mechanical power input provided by the radiation pressure force, $\hbar G\langle|\alpha|^2\dot{x}\rangle$, in terms of $G\bar{A}$ [16]. This yields $\gamma = 2\mathcal{P}\Omega\pi_2 - \Gamma$ and $(G\bar{A}/\kappa)^2 = \gamma\Omega/(-2\pi_4\mathcal{P}\kappa^2)$, where the dimensionless coefficients $\pi_2(\Delta/\Omega, \kappa/\Omega)$ and $\pi_4(\Delta/\Omega, \kappa/\Omega)$ only depend on the rescaled detuning and cavity decay rate. $\mathcal{P} = \hbar G^2\alpha_{\max}^2/m\Omega^3$ is the rescaled laser input power. Note that the oscillation frequency in the Hopf model will be renormalized by the "optical spring effect" [8].

We start our discussion by considering phase-locking to an external force $F(t) = F_0\sin(\omega_F t)$. To this end we time-average Eq. (3), keeping only the slow dynamics, under the assumption $\omega_F \approx \Omega$. This results in the Adler equation $\delta\dot{\varphi} = \delta\Omega + K_F\sin(\delta\varphi)$, where $\delta\varphi = \varphi(t) + \omega_F t$, $\delta\Omega = \omega_F - \Omega$, and $K_F = F_0/2m\Omega\bar{A}$. Direct numerical simulation confirms the good agreement between the microscopic optomechanical dynamics and the simplified descriptions, i.e., Hopf Eqs. (3) and (4) and the Adler phase equation (analogous to the Kuramoto-type equations studied below); see Fig. 2. The phase φ is extracted from the complex amplitude of motion, $\beta \equiv x + i\dot{x}/\Omega = |\beta|e^{i\varphi}$. Phase locking sets in when $\delta\dot{\varphi} = 0$ has a solution, i.e., for $|\delta\Omega| \le K_F$, resulting in an "Arnold tongue" [see Fig. 2(c)].

We now turn to the dynamics of N mechanically coupled cells. Optical coupling will be discussed below. Each cell is described by Eqs. (1) and (2). To these equations, we add mechanical couplings where we consider a general coupling matrix set by individual spring constants k_{ij}: $m\ddot{x}_i = \ldots + \sum_{j\neq i}k_{ij}(x_j - x_i)$. In the Hopf model with phase dynamics $\varphi_i(t)$ and amplitude dynamics $A_i(t)$ according to Eqs. (3) and (4), this yields a force $F_i = \sum_{j\neq i}k_{ij}A_j\cos(\varphi_j)$ on cell i.

To arrive at the time-averaged dynamics for the phase exclusively, it is necessary to go further than before, carefully respecting the amplitude dynamics $A_i(t) = \bar{A}_i + \delta A_i(t)$ in the phase equation (see [25,26] for further examples where the amplitude dynamics is crucial). The formal solution for $\delta A_i(t)$ is $\delta A_i(t) = \int_{-\infty}^{t} e^{-\gamma(t-t')}\tilde{f}_i(t')dt'$, where $\tilde{f}_i(t) = \sum_{j\neq i}(k_{ij}/m_i\Omega_i)(\bar{A}_j + \delta A_j(t))\cos\varphi_j(t)\sin\varphi_i(t)$. In the following, we consider small couplings, where $\delta A_i \ll \bar{A}_i$. In this case we can evaluate the formal solution $\delta A_i(t)$ and find an expression $\delta A_i(\varphi_1, \ldots, \varphi_N)$. Thus, we can eliminate the amplitude dynamics from the equations for $\dot{\varphi}_i$, where we expand A_j/A_i to leading order. Finally, we perform a time average, keeping only the slow phase dynamics near frequencies 0 and $\pm|\Omega_j - \Omega_i|$. We thus arrive at an effective Kuramoto-type model for coupled optomechanical Hopf oscillators,

$$\begin{aligned}\partial_t\varphi_i = &-\Omega_i + \sum_{j\neq i}\frac{\xi_{ij}}{2}\cos(\varphi_j - \varphi_i)\\ &+ \sum_{j\neq i}\sum_{k\neq j}\frac{\xi_{ij}\xi_{jk}}{8\gamma}(\sin(2\varphi_j - \varphi_k - \varphi_i) - \sin(\varphi_k - \varphi_i))\\ &+ \sum_{j\neq i}\sum_{k\neq i}\frac{\xi_{ij}\xi_{ik}}{8\gamma}\sin(\varphi_k + \varphi_j - 2\varphi_i)\end{aligned} \tag{5}$$

where $\xi_{ij} = k_{ij}\bar{A}_j/m_i\Omega_i\bar{A}_i$.

For two coupled cells ($N = 2$, $k_{ij} = k$), Eq. (5) yields for the phase difference $\delta\varphi = \varphi_2 - \varphi_1$:

$$\delta\dot{\varphi} = -\delta\Omega - C\cos(\delta\varphi) - K\sin(2\delta\varphi). \tag{6}$$

In contrast to the standard Kuramoto model, $2\delta\varphi$ appears, which will lead to both in-phase and antiphase synchronization. This corresponds to two distinct minima in the effective potential that can be used to rewrite Eq. (6): $\delta\dot{\varphi} = -U'(\delta\varphi)$. The description in terms of a phase particle sliding down a washboard potential [Fig. 3(a)] is similar to that of an overdamped Josephson junction driven by a current bias set by $\delta\Omega$. The coupling constants are given by $C = (\xi_{12} - \xi_{21})/2$, $K = (\xi_{12} + \xi_{21})^2/8\gamma$. In the following we focus on the case of nearly identical cells

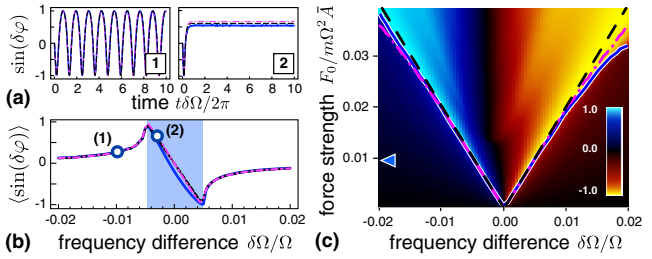

FIG. 2 (color online). Phase locking of an optomechanical cell to an external force. (a) Phase lag $\delta\varphi$ between oscillations and force, outside (left) and inside (right) the phase-locked regime. (b) Time-average $\langle\sin\delta\varphi\rangle$ as function of $\delta\Omega$ comparing optomechanics (blue, solid) against the Hopf model (magenta, dash-dot) and the Adler phase equation (black, dash). Colored region indicates $\delta\dot{\varphi} = 0$. (c) "Arnold tongue"; $\langle\sin\delta\varphi\rangle$ in the force vs frequency difference plane. Lines show the transition towards phase-locking; styles as in (b). The triangle labels F_0 in (b). (Microscopic cell parameters: $\Delta/\Omega = 1$, $\kappa/\Omega = 1$, $\Gamma/\Omega = 0.01$, $\mathcal{P} = \hbar G^2\alpha_{\max}^2/m\Omega^3 = 0.36$).

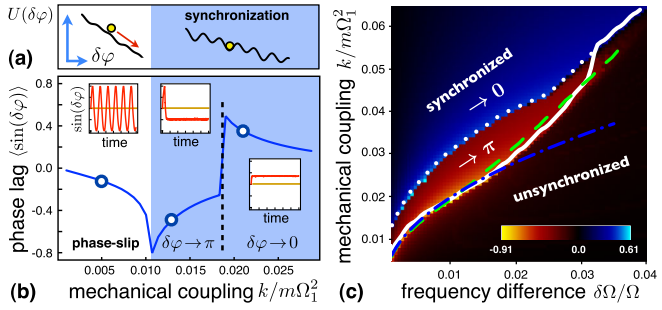

FIG. 3 (color online). Phase locking of two mechanically coupled optomechanical cells. (a) Phase particle in the effective Kuramoto potential $U(\delta\varphi)$; desynchronized (left), phase-locked (right). (b) Time-average $\langle \sin\delta\varphi \rangle$ as function of mechanical coupling k. When k exceeds a threshold k_c (colored region), the phase difference $\delta\varphi(t)$ between the oscillations locks to a constant value despite different bare mechanical frequencies, here $\delta\Omega = 0.003\Omega_1$. Both in-phase and antiphase synchronization regimes are observed. (c) $\langle \sin(\delta\varphi) \rangle$ in the plane coupling k vs frequency difference $\delta\Omega$, including a comparison of the critical coupling k_c (white, solid) with the one from a Hopf model with one fit parameter (green, dash) and the effective Kuramoto-type model (blue, dash-dot). (Cell parameters as in Fig. 2).

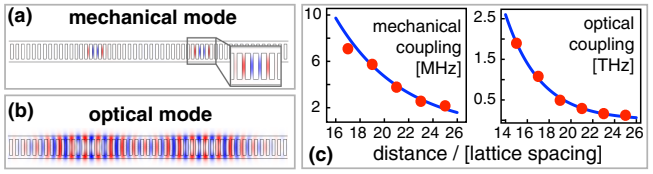

FIG. 4 (color online). FEM simulation for two coupled cells localized on the same beam in an optomechanical crystal setup [cf. Figure 1(a)]. Geometrical parameters for each individual cell as in Ref. [9]. (a) Horizontal displacement of vibrational "pinch" modes. (b) Transverse electric fields of optical modes. (c) The intercell couplings decay exponentially as a function of the cells' distance.

where the coupling C can be neglected ($C/\delta\Omega = k/2m\Omega^2 \ll 1$), and $K = k^2/2m^2\Omega^2\gamma$.

To test whether the features predicted by Eq. (6) are observed in the full optomechanical system, we directly simulate the motion and increase the coupling k for a fixed frequency difference $\delta\Omega = \Omega_2 - \Omega_1$. The results are displayed in Fig. 3(b). Beyond a threshold k_c, the frequencies and phases lock, indicated by a kink in $\langle \sin\delta\varphi \rangle$. As the coupling increases further, the phases are pulled towards each other, so $|\delta\varphi|$ decreases. As predicted, there is both synchronization towards $\delta\varphi \to 0$ and $\delta\varphi \to \pi$. The dependence of the threshold k_c on the frequency difference $\delta\Omega$ is shown in Fig. 3(c). The observed behavior $k_c \propto \sqrt{\delta\Omega}$ at small $\delta\Omega$ is correctly reproduced by the effective Kuramoto-type model, Eqs. (5) and (6). For $\delta\Omega > \gamma$ deviations occur via terms of higher order in $\delta\Omega/\gamma$, starting with $-(\delta\Omega/\gamma)K\cos(2\delta\varphi)$ in Eq. (6). These produce a linear slope $k_c \propto \delta\Omega$; see Fig. 3(c).

We point out that the simulation in Fig. 3 shows results for experimentally realistic parameters (see discussion below) using a laser input power well above the bifurcation threshold. This allows one to observe the essential features in an appropriate range of frequency detuning $\delta\Omega$. To achieve quantitative agreement of the Hopf model with microscopic results in Fig. 3, its parameter γ is treated as an adjustable parameter (here $\gamma = 0.02\ \Omega$). Whether the system synchronizes towards $\delta\varphi \to 0$ or $\delta\varphi \to \pi$ also depends on the initial conditions. Our simulations initially start with a system at rest and consider an instantaneous switch-on of the laser input power.

In terms of experimental realization, photonic "optomechanical" crystals [8,9] offer a novel promising way to build optomechanical arrays [Fig. 1(a)]. To consider coupled cells in such designs, we use finite element methods (FEM) to simulate two identical cells arranged on the same beam [Figs. 4(a) and 4(b)]. Figure 4(c) shows the optical and mechanical couplings mediated by the geometry. This indicates $k/m\Omega^2 \lesssim 0.01$, which we use in our dynamical simulations, together with cell parameters reported in [8,9]. Because of the relatively strong optical coupling ($\sim$ THz), distinct OMs in the individual cells can only be achieved by patterning them to have frequencies sufficiently different to prevent hybridization. This requires different laser colors to address each cell.

In experiments, a convenient observable would be the RF frequency spectrum of the light intensity emanating from the cells, $|\alpha|^2(\omega)$. Figure 5(a) shows the spectrum as a function of frequency difference $\delta\Omega$ (additional peaks are produced by nonlinear mixing). The comparison to results from a simulation of Eq. (5) illustrates an excellent

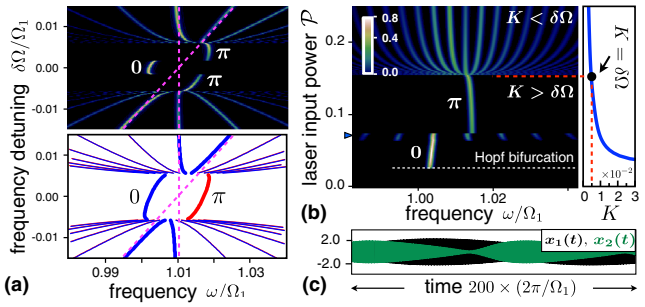

FIG. 5 (color online). Mechanical frequency spectra $I(\omega)$ of intensity fluctuations, $I(t) = |\alpha_1(t)|^2 + |\alpha_2(t)|^2$, for two mechanically coupled cells. (a) Frequency locking upon changing the detuning $\delta\Omega = \Omega_2 - \Omega_1$ between the mechanical frequencies (magenta, dash). Top: spectrum $I(\omega)$ from optomechanics. Bottom: spectral peaks of $\sum_i \cos(\varphi_i(t))$ from a simulation of the effective Kuramoto-type model, Eq. (5). Depending on initial conditions we find in-phase (blue) and antiphase (red) synchronization. ($k/m\Omega_1^2 = 0.015$). (b) Spectrum $I(\omega)$ and effective Kuramoto coupling K [Eq. (6)] vs laser input power. ($k/m\Omega_1^2 = 0.01$, $\delta\Omega = 0.005\Omega_1$). (c) Example of trajectories $Gx_i(t)/\kappa$ displaying strong amplitude modulation, not described by the Kuramoto model [at power indicated by the triangle in (b)]. (Color scale indicates $|I(\omega)|$ in units of the peak height at $\omega = 0$ for a system with $G = 0$; δ peaks are broadened for clarity; parameters as in Figs. 2 and 3)

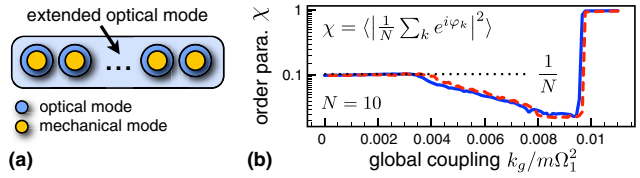

FIG. 6 (color online). Optomechanical array with global coupling. (a) Schematic: global coupling scheme. (b) Order parameter χ vs coupling k_g for an array of $N = 10$ cells, comparing optomechanics (blue) to results from the effective Kuramoto-type model Eq. (5) (red, dashed) using one fit parameter, $\gamma = 0.036\ \Omega$. (Ω_i are chosen equidistant from $0.98\ \Omega$ to $1.02\ \Omega$.)

agreement with the effective Kuramoto-type model. Around $\delta\Omega = 0$, we recover in-phase and antiphase synchronization that differ in the synchronization frequency, $\bar{\Omega}(\pi) - \bar{\Omega}(0) = (\xi_{12} + \xi_{21})/2 \simeq k/m\Omega$. Experimentally, mechanical frequencies can be tuned via the optical spring effect. The most easily tunable parameter however is the laser drive power ($\propto \alpha_{\mathrm{max}}^2$); see Fig. 5(b). Synchronization sets in right at the Hopf bifurcation while at higher drive, we find a transition towards desynchronization. Again, this can be explained from our analytical results. We know that γ increases away from the Hopf bifurcation (i.e., for higher drive), leading to a concomitant decrease in the effective Kuramoto coupling $K \propto 1/\gamma$ [inset Fig. 5(b)], and finally a loss of synchronization ($K < \delta\Omega$). In some regimes, we observe strong amplitude modulation where the Kuramoto model fails [Fig. 5(c)].

For large arrays ($N \gg 2$), one might be interested in a long-range, global coupling between cells ($k_{ij} = k_g$). This can be designed in terms of a fast ($\kappa_{\mathrm{ext}} \gg \Omega_i$), extended optical mode α_{ext}, coupled to the mechanics of each cell, [Fig. 6(a)]. The light-field intensity is then modulated by $\sum_j x_j$, and the light force thus generates a global mechanical coupling $k_g = -\hbar G^2 |\bar{\alpha}_{\mathrm{ext}}|^2 \frac{8\Delta}{4\Delta^2 + \kappa_{\mathrm{ext}}^2}$, where $|\bar{\alpha}_{\mathrm{ext}}|^2$ is the average number of circulating photons tunable via the laser power. $k_{ij} = k_g$ enters Eq. (5).

Figure 6(b) shows results on the order parameter $\chi = \langle |\frac{1}{N}\sum_k e^{i\varphi_k}|^2 \rangle$ for an array of ten globally coupled optomechanical cells [Fig. 6(a)]. For small coupling, each cell oscillates independently, the phases φ_k are random, and thus $\chi = 1/N$. For larger coupling, we find a regime where the phases are not fully phase locked but the phase factors become anticorrelated, decreasing χ. At large k_g there is a transition to phase locking, where finally all cells are synchronized with $\chi \simeq 1$. All these features are reproduced nicely by the effective Kuramoto-type model, Eq. (5), [Fig. 6(b)].

To conclude, we have introduced optomechanical arrays as a new system to study collective oscillator dynamics, with room-temperature operation in integrated nanofabricated circuits and with novel possibilities for readout and control, complementing existing research on Josephson arrays [22], laser arrays [23] and other nanomechanical structures [24,27]. Recent experiments on 2D optomechanical crystals [28] could form the basis for investigating collective dynamics in 2D settings with various coupling schemes. Applications in metrology and time-keeping may benefit from phase noise suppression via synchronization [29]. Variations of the optomechanical arrays investigated here may also be realized in other designs based on existing setups, like multiple membranes in an optical cavity [30] or arrays of toroidal microcavities [2,5].

We thank O. Painter, H. Tang, and J. Parpia for fruitful discussions, and GIF as well as DFG (Emmy-Noether program, NIM) and DARPA ORCHID for funding.

[1] F. Marquardt and S. M. Girvin, Physics **2**, 40 (2009).
[2] A. Schliesser *et al.*, Nature Phys. **5**, 509 (2009).
[3] S. Gröblacher *et al.*, Nature Phys. **5**, 485 (2009).
[4] W. Marshall *et al.*, Phys. Rev. Lett. **91**, 130401 (2003).
[5] G. Anetsberger *et al.*, Nature Phys. **5**, 909 (2009).
[6] P. Verlot *et al.*, Phys. Rev. Lett. **102**, 103601 (2009).
[7] J. D. Teufel *et al.*, Nature Nanotech. **4**, 820 (2009).
[8] M. Eichenfield *et al.*, Nature (London) **459**, 550 (2009).
[9] M. Eichenfield *et al.*, Nature (London) **462**, 78 (2009).
[10] D. Chang *et al.*, New J. Phys. **13** 023003 (2011).
[11] M. Li *et al.*, Nature (London) **456**, 480 (2008).
[12] M. Li, W. H. P. Pernice, and H. X. Tang, Nat. Photon. **3**, 464 (2009).
[13] C. Höhberger and K. Karrai, *Nanotechnology 2004, Proceedings of the 4th IEEE Conference on Nanotechnology* (2004), p. 419.
[14] T. Carmon *et al.*, Phys. Rev. Lett. **94**, 223902 (2005).
[15] T. J. Kippenberg *et al.*, Phys. Rev. Lett. **95**, 033901 (2005).
[16] F. Marquardt, J. G. E. Harris, and S. M. Girvin, Phys. Rev. Lett. **96**, 103901 (2006).
[17] M. Ludwig, B. Kubala, and F. Marquardt, New J. Phys. **10**, 095013 (2008).
[18] C. Metzger *et al.*, Phys. Rev. Lett. **101**, 133903 (2008).
[19] A. Pikovsky, M. Rosenblum, and J. Kurths, *Synchronization: A Universal Concept in Nonlinear Sciences* (Cambridge University Press, Cambridge, England, 2001).
[20] Y. Kuramoto, in *International Symposium on Mathematical Problems in Theoretical Physics*, (Springer, New York, 1975), Vol. 39, pp. 420.
[21] J. A. Acebrón *et al.*, Rev. Mod. Phys. **77**, 137 (2005).
[22] K. Wiesenfeld, P. Colet, and S. H. Strogatz, Phys. Rev. Lett. **76**, 404 (1996).
[23] G. Kozyreff, A. G. Vladimirov, and P. Mandel, Phys. Rev. Lett. **85**, 3809 (2000).
[24] M. C. Cross *et al.*, Phys. Rev. Lett. **93**, 224101 (2004).
[25] D. Aronson, G. Ermentrout, and N. Kopell, Physica (Amsterdam) **41D**, 403 (1990).
[26] P. C. Matthews, R. E. Mirollo, and S. H. Strogatz, Physica (Amsterdam) **52D**, 293 (1991).
[27] M. Zalalutdinov *et al.*, Appl. Phys. Lett. **83**, 3281 (2003).
[28] A. H. Safavi-Naeini *et al.*, Appl. Phys. Lett. **97**, 181106 (2010)
[29] S. Tallur *et al.*, *Frequency Control Symposium (FCS), 2010 IEEE International* (IEEE, 2010), p. 268. .
[30] J. D. Thompson *et al.*, Nature (London) **452**, 72 (2008).